Human Thermal Load of Cfb Climate Summer Weather Based on the Concept of Required Skin Evaporation

Ferenc Ács[A*]**, Erzsébet Kristóf**[A]**, Annamária Zsákai**[B]

[A] Eötvös Loránd University, Faculty of Science, Department of Meteorology, Pázmány Péter sétány 1/A., Budapest, Hungary; ORCID FA: 0000-0002-1611-6839; EK: 0000-0001-9892-9552
[B] Eötvös Loránd University, Faculty of Science, Department of Human Anthropology, Pázmány Péter sétány 1/C, Budapest, Hungary; ORCID AZ: 0000-0001-8880-2056

Abstract

We analyzed the human thermal load of summer weather in the Cfb climate based on the results of a new model based on the human body energy balance equation and the skin surface evaporation gradient formula. The active surface of the model is the skin surface, the person is lying in a resting position, its skin type is Fitzpatrick skin type IV. For that purpose, longitudinal research method was performed in 2022 in Martonvásár, Hungary (East-Central Europe), comprising 331 observations in which weather conditions and thermal sensation types were recorded simultaneously. The main observation is that in warm climates and/or weather situations, the amount of thermal load can be very simply characterized by latent heat flux density values of the skin evaporation. From a human point of view, the most important characteristics of summer weather in the Cfb climate are as follows: 1) The latent heat flux density of skin surface evaporation varied between 10 and 300-350 Wm^{-2}, while the operative temperature ranged between 25 °C and 80 °C. 2) The relationship between skin surface evaporative resistance and operative temperature can be characterized by an exponential function. In cases of thermal sensation type "neutral", skin surface evaporative resistance values are mostly above 0.5 hPa·m^2·W^{-1}. Observations made by people with different skin types are essential to generalize the results.

Keywords: Cfb climate; summer weather; human thermal load; required skin evaporation; evaporative resistance of skin

Introduction

Experiencing thermal load is deeply subjective (von Humboldt, 1845), especially during the summer season when the excess of heat approaches its maximum values (Hantel & Haimberger, 2016). Table 1 gives a brief overview of the climatological methods for characterizing heat excess. As we see, the examination of heat-excess can be linked, but does not necessarily have to be linked to living beings. Even today, the statistical analysis of data in space and time is a frequently used methodology. The analysis of heatwaves and warm extremes has grown in popularity recently (Basarin et al., 2020). The vast majority of the studies are not related to the living world (Bokros & Lakatos, 2022; Megyeri-Korotaj et al., 2023; Boras et al., 2022), but it should be emphasized that several studies have dealt with the investigation of the relationship between heat waves and mortality, or illnesses (Fouilett et al.,

---

* Corresponding author: Ferenc Ács; e-mail: acs@caesar.elte.hu

2006; Páldy et al., 2018; Khosla & Guntupalli, 1999). Among the many climate indices, the tourism climate index (TCI) should be mentioned (Mieczkowski, 1985). The index is applied to actual conditions and tries to express the simultaneous, integrated effect of several meteorological elements on the tourist's comfort in a quantified form. It should be mentioned that there are newer modified versions of this index (Kovács et al., 2017). However, in TCI the human being is not specified.

Table 1. Brief overview of the climatological methods for characterizing environmental heat excess.

Methods	Chosen features		
	Climatic characteristic	**Living being**	**The size of the living community**
Data analysis	heat waves, warm extremes, climate indices		
Heat index	thermal load in warm period	human	group of people
Köppen's method	seasonality	vegetation	biome size
Physiologically equivalent temperature	thermal load	human	group of people
Universal Thermal Climate Index	thermal stress	human	group of people
Concept of the required skin evaporation	thermal load in warm period	human	individuals

In contrast to extreme events and targeted applications, climate has annual and/or seasonal characteristics. The most common method for describing the annual characteristics of the climate (averages and fluctuations) is the method of the Köppen (Köppen, 1936). Köppen's method is vegetation-based (Köppen, 1900), it is designed for biome-scale applications. In Köppen's climate formula, the 3rd symbol (*a* – hot summer, *b* – warm summer, *c* – cool summer, *d* – extremely continental) characterizes the type of summer heat availability (Kottek et al., 2006), which is independent from the type of the biome. In summary: Köppen's method do characterize summer, but only for orientation.

In contrast to Köppen's method, the heat index (HI) only focuses on the summer period. The thermal load subject is a human. This "standard human" represents a group of people. In the case of HI, it is 170 cm tall, weighs 67 kg, walks in the shade at a speed of 1.5 ms^{-1} in a light breeze of 2.7 ms^{-1}, wearing long pants and a short-sleeved shirt (Mohan et al., 2014). The human characteristics are not taken into account in calculating HI values, but they are included implicitly in the categorization of heat risk. The method requires only 2 input data: air temperature and relative humidity. It is described and applied, for instance, in Hungary in the period 1971-2020 by Bátori (2022). In the United States, HI is also used in meteorological operational practice.

In our days and age, the use of energy balance-based methods in biometeorological applications has become widespread (Potchter et al., 2018). By calculating the energy balance of the human body covered with clothing, the effect of human characteristics on thermal load can also be analyzed. Thus, these methods make it possible to simulate the subjective

experience of the climate (von Humboldt, 1845). Among these, the two most popular methods are the PET (Physiologically Equivalent Temperature) and UTCI (Universal Thermal Climate Index) methods. Both methods use "standardized human", the advantage is that the thermal load is to be applied to a group of people, the disadvantage is that the subjective nature disappears in the characterization of the human-climate relationship. We emphasize that the climate is what we perceive it to be. It should be noted that the "standardized human" in the PET, UTCI, and HI methods are different and tend to be men. In the Austria-Hungary region, the PET index was used most often (Matzarakis et al., 2005; Matzarakis & Gulyás, 2006). There is also a study that focus on estimating the thermal load in the summer months (Gulyás & Matzarakis, 2009). However, the assessment of summer warm extremes using the PET or UTCI methods is becoming widespread (Basarin et al., 2020; Błazejczyk et al., 2014; Pecelj et al., 2019).

The simplest energy balance-based method is the one that uses the concept of required skin evaporation (Parsons, 1997). The method can only be used in climatic or weather conditions that cause excess heat. If there is no heat storage, then the skin evaporation (practically sweating as his value changes) that compensates for the excess heat is the required skin evaporation, and therefore this must be determined as a residual term in the energy balance equation. Although the method is very simple, it is less widely used due to the more complicated determination of other terms that make up the energy balance. To the best of our knowledge, there are no studies dealing with quantification of summer excess heat based on the concept of required skin evaporation. This study aims to fill this gap.

The specific objectives of this study are as follows: to characterize the relationship between 1) latent heat flux density of required skin evaporation (λE_{tot}^{req}) and operative temperature (T_o), 2) λE_{tot}^{req} and thermal perception types and 3) skin evaporative resistance (r_{skin}) and T_o. 4) We also aimed to test the behavior of the model to changes in skin albedo. Finally, 5) we also talk about the applicability of the model. It should be noted that the longitudinal experiment is performed in lowland area of the Pannonian region (Hungary, Martonvásár) in the summer of 2022. The person was wearing minimal summer clothing and was always in a lying position.

Methodology

The study is conducted using the longitudinal research method. An important part of the study is the observation of thermal perception. Since thermal perception observations occurred, information about skin type is also essential. Fitzpatrick skin typing method is used for characterizing skin type. Human thermal load is characterised by latent heat flux density of the required skin evaporation. Thermal perception type results were derived by strict application of an observation protocol. Finally, thermal load and thermal sensation type results are carefully checked and filtered. The listed methodological elements are now described one by one.

Longitudinal observations

The basic methodology of this study is longitudinal observation. One person (hereafter observer) performed long-term, concurrent thermal load estimations and thermal perception observations in the summer of 2022. There were a total of 331 observations. The methodological elements used by the observer during each observation are described below.

Basic equations of the model

If there is no heat storage (constant surface temperature), the energy balance of the skin surface of the human body can be written as follows,

$$R_n + M - \lambda E_r - H_r - W - H_s - \lambda E_{tot} = 0, \qquad (1)$$

where R_n is the net radiation energy flux density [Wm^{-2}], M is the metabolic energy flux density [Wm^{-2}], λE_r is respiratory latent heat flux density [Wm^{-2}], H_r is respiratory sensible heat flux density [Wm^{-2}], W is mechanical work flux density [Wm^{-2}], which refers to the activity being carried out, H_S is sensible heat flux from the skin surface [Wm^{-2}] and λE_{tot} is latent heat flux density of the skin evaporation [Wm^{-2}]. In this model, M = 55 Wm^{-2} and W = 0 Wm^{-2} since the person is in a lying position.

The latent heat flux density of skin surface evaporation can also be expressed using the gradient formula,

$$\lambda E_{tot} = \frac{\frac{\rho \cdot c_p}{\gamma} \cdot [e_S(T_s) - e_a]}{r_{skin} + r_{Ha}}, \qquad (2)$$

where ρ is air density [kgm^{-3}], c_p is specific heat at constant pressure [Jkg^{-1}°C^{-1}], γ is psychrometric constant [hPa°C^{-1}], T_{skin} is skin surface temperature (34 °C) (Campbell & Norman, 1997), $e_S(T_{skin})$ [hPa] is saturation vapor pressure at T_{skin}, e_a is actual vapor pressure [hPa], r_{skin} is the evaporative resistance of skin surface [sm^{-1}] and r_{Ha} is the aerodynamic resistance for expressing convective heat exchange effect [sm^{-1}].

Applying the model conditions, we can express λE_{tot} and r_{skin} from equations (1) and (2),

$$\lambda E_{tot} = R_n + M - \lambda E_r - H_r - H_s, \qquad (3)$$

$$r_{skin} = \frac{\frac{\rho \cdot c_p}{\gamma} \cdot [e_S(T_s) - e_a]}{R_n + M - \lambda E_r - H_r - H_s} - r_{Ha}, \qquad (4)$$

When estimating λE_{tot}^{req}, we use not only equation (3), but also equation (4). Namely, $\lambda E_{tot}^{req} = \lambda E_{tot}$ if $r_{skin} \geq 0$.

Parametrizations
Radiation: R_n is parameterised as simply as possible,

$$R_n = S \cdot (1 - \alpha_{skin}) + \epsilon_a \sigma T_a^4 - \epsilon_{skin} \sigma T_{skin}^4, \qquad (5)$$

where *S* is incoming solar radiation [Wm^{-2}], σ is Stefan-Boltzmann constant [Wm^{-2}K^{-4}], ϵ_a is emissivity of the cloudy sky, T_a is air temperature [°C], α_{skin} is skin surface albedo and ϵ_{skin} is emissivity of the skin surface. In this study, α_{skin} = *0.27* (concentration of melanosomes in epidermis is 2.5%, (Nielsen et al., 2008)), ϵ_{skin} = 1. S is estimated according to the work of Ács et al. (2025),

$$S = Q_0 \cdot [\alpha + (1 - \alpha) \cdot rsd], \qquad (6)$$

where Q_0 is solar radiation constant [MJ·m^{-2}·hour^{-1}] referring to clear sky conditions and a 1-hour time period, α is the corresponding dimensionless constant referring to the same hour

and *rsd* is relative sunshine duration. ϵ_a depends on clear sky emissivity ϵ_{cs} and cloudiness N (0 for cloudless and 1 for completely overcast conditions),

$$\epsilon_a = \epsilon_{cs} \cdot (1 - N^{1.6}) + 0.9552 \cdot N^{1.6}, \quad (7)$$

$$\epsilon_{cs} = 0.51 + 0.066 \cdot \sqrt{e_a}. \quad (8)$$

ϵ_{cs} and ϵ_a are given according to Brunt (1932) and Konzelmann et al. (1994), respectively. Heat flux densities: λE_r and H_r depend upon M, they are parameterized according to Fanger (1970) as follows,

$$\lambda E_r = 1.72 \cdot 10^{-5} \cdot M \cdot (5867 - e_{ap}), \quad (9)$$

$$H_r = 1.4 \cdot 10^{-3} \cdot M \cdot (T_s - T_a), \quad (10)$$

where e_{ap} is actual vapor pressure [Pa]. H_S is expressed as

$$H_s = \rho \cdot c_p \cdot \frac{T_s - T_a}{r_{Ha}}, \quad (11)$$

r_{Ha} depends upon wind velocity (Campbell & Norman, 1997),

$$r_{Ha}[sm^{-1}] = 7.4 \cdot 41 \cdot \sqrt{\frac{D}{U_{0.5}}}, \quad (12)$$

where D is the diameter of the cylindrical body used to approach the body of the observer (Campbell & Norman, 1997), $U_{0.5}$ is the wind speed at 0.5 m height (sunbed height).

Operative temperature: It depends upon air temperature, net radiation flux density and wind speed (Campbell & Norman, 1997) as follows,

$$T_o = T_a + \frac{R_n}{\rho \cdot c_p} \cdot r_{Ha}. \quad (13)$$

Estimation of thermal sensation
Each thermal sensation observation is performed according to the following observation protocol: 1) the observer always started the observation with a "neutral" thermal sensation, that is, he started from a place of about 24–26 °C2) all observations were made wearing the same sports garment, which was (the observer was male) put on immediately before starting the observation (we emphasize that the observer was not wearing other clothing than the sports garment), 3) the observer always performed the observation in a supine position for at least 10 minutes lying on the sunbed shown in Figure 1, 4) the beach pillow was always stored in a place where the thermal sensation was "neutral" and 5) all data were registered immediately (observed thermal sensation type and the meteorological variables) after the observation.

Figure 1. The observer during a thermal perception observation. His anthropometric data are as follows: body mass 89 kg, body height 190 cm, and age 67 years

As we can see, we used the human body's thermal sensors as a monitoring tool. This has advantages and disadvantages. A major advantage is that the thermal sensation is human-based, as every living being (species, individual) experiences and perceives the same thermal supply differently. Its disadvantage is that it is difficult to quantify, i.e. it is less exact, and it is subjective. The variability of subjectivity is not great, we can state this based on our experience. The fact that the thermal sensation is described in words rather than numbers should not be considered a disadvantage.

Management of thermal sensation and thermal load data
Weather and thermal sensation data are collected concurrently. The following data management protocol was applied after each observation: 1) Human thermal load characteristics (latent heat flux density of the skin evaporation and evaporative resistance of the skin) were calculated immediately after each observation, 2) the cases when the method was not applicable ($r_{skin} < 0$) were eliminated, 3) the consistency between thermal load characteristics and thermal perception types observed was checked and 4) we have always tried to interpret the relationships that cause thermal load. The printed list of output variables calculated with the model is shown in Figure 2.

Y	M	D	TA2	RN	S		N		TO						HS		ETOT			RSKIN	THERMAL PERCEPTION TYPE
22	5	12	24.2	443.0	822.2	1.4	2.5	0.0	86.4	115.8	40.9	154.	249.	186.	39.7	3.4	47.4	431.9	35.98	-0.051	-0.33 WARM, LYING SWEAT
22	5	13	24.8	103.1	276.2	1.7	2.5	0.9	48.6	44.1	31.1	711.	226.	186.	39.7	3.3	49.0	90.5	34.72	0.262	1.69 NEUTRAL, LYING
22	5	14	23.5	468.7	822.2	1.9	2.5	0.7	88.8	106.7	41.0	168.	214.	186.	39.7	3.7	59.1	445.5	40.45	-0.025	-0.16 WARM, LYING
22	5	15	20.7	236.8	580.3	1.9	5.5	0.0	65.0	62.7	32.6	373.	214.	126.	39.7	3.8	74.9	197.7	39.76	0.086	0.55 SLIGHTLY WARM, LY
22	5	15	25.7	463.1	863.1	1.4	3.3	0.0	88.3	121.5	42.5	163.	249.	162.	39.7	3.6	40.1	459.1	40.31	-0.047	-0.30 VERY WARM, LYING,
22	5	15	25.6	147.3	431.4	0.8	1.7	0.0	54.3	65.9	33.2	490.	330.	226.	39.7	3.6	30.7	152.6	40.39	0.087	0.56 SLIGHTLY WARM, LY
22	5	16	26.8	370.9	709.4	1.4	2.5	0.2	79.4	103.5	40.9	189.	249.	186.	39.7	3.4	34.8	372.4	38.04	-0.032	-0.21 VERY WARM, LYING,
22	5	16	27.2	124.7	340.8	1.1	1.9	0.5	51.4	56.3	33.6	524.	281.	214.	39.7	3.3	29.1	131.9	37.32	0.131	0.85 SLIGHTLY WARM, LY
22	5	18	19.0	427.5	863.1	1.4	2.8	0.2	84.9	107.4	36.7	207.	249.	176.	39.7	4.2	72.5	390.5	43.52	-0.023	-0.15 VERY WARM, LYING,
22	5	20	27.5	456.5	822.2	1.1	2.5	0.1	87.7	134.0	43.6	148.	281.	186.	39.7	3.3	27.9	465.1	37.04	-0.072	-0.46 VERY WARM, LYING,
22	5	20	28.2	94.4	254.9	2.2	4.7	0.8	47.5	43.8	33.3	719.	199.	136.	39.7	3.2	35.2	95.7	37.13	0.281	1.81 NEUTRAL, LYING
22	5	20	29.3	9.5	195.3	0.8	1.7	0.0	35.4	31.9	30.8	2315.	330.	226.	39.7	3.1	17.2	28.9	36.07	1.071	6.91 NEUTRAL, LYING
22	5	20	28.9	176.8	431.4	0.8	1.9	0.0	58.0	77.3	36.6	351.	330.	214.	39.7	3.2	18.6	194.7	36.86	0.012	0.07 WARM, LYING
22	5	21	26.5	275.6	591.9	1.4	3.1	0.0	69.4	83.5	37.9	260.	249.	167.	39.7	3.4	36.3	275.6	38.65	0.006	0.04 WARM, LYING, NYIR
22	5	22	22.4	414.6	822.2	2.3	3.5	0.1	83.7	89.3	38.8	205.	194.	158.	39.7	3.9	71.9	378.6	41.81	0.006	0.04 WARM, LYING, NYIR
22	5	22	23.0	276.6	591.9	1.4	2.8	0.5	69.5	80.2	35.4	296.	249.	176.	39.7	3.8	53.2	259.3	41.39	0.025	0.16 WARM, LYING

Figure 2. A cutout image of the model results. Notations: Y - year, M - month, D - day, TA2 - air temperature [°C], RN - radiation balance [Wm^{-2}], S - global radiation [Wm^{-2}], N - cloudiness, TO - operative temperature [°C], HS - sensible heat flux density from the skin surface [Wm^{-2}], ETOT - latent heat flux density of skin surface evaporation [Wm^{-2}] and RSKIN - skin surface resistance to evaporation [$hPa \cdot m^2 \cdot W^{-1}$]

The designation of the selected variables can be found in the title of Figure 2. Looking at Figure 2, we can notice negative r_{skin} values (penultimate column).

Fitzpatrick skin typing method
Fitzpatrick skin typing method (Fitzpatrick, 1975) is a well-known method for classifying human skin types. It uses three input variables: skin color (a numerical value on a scale 1-30), eye color (a numerical value on a scale 1-16) and hair color when the person is young (a numerical value on a scale 1-10). The classification is done based on the sum of the points. The scores and Fitzpatrick skin types are presented in Table 2.

Table 2. Fitzpatrick skin types

Type	Scores	Skin color characterization	Skin tone
I	0-6	Caucasian, blond/red hair, freckles, fair skin, blue eyes	very fair
II	6-13	Caucasian	fair
III	14-20	Darker Caucasian, light Asian	fair to medium
IV	21-27	Mediterranean, Asian, Hispanic	medium

V	28-34	Middle Eastern, Latin, light-skinned black, Indian	olive to dark
VI	35+	Dark-skinned black	very dark

Location

The region and the location are presented in Figure 3. Town Martonvásár is located in the lowland area of Hungary. Within Martonvásár, the observations took place in the garden of a family house, the basic tools required for the observation are also shown in Figure 3 (on the right).
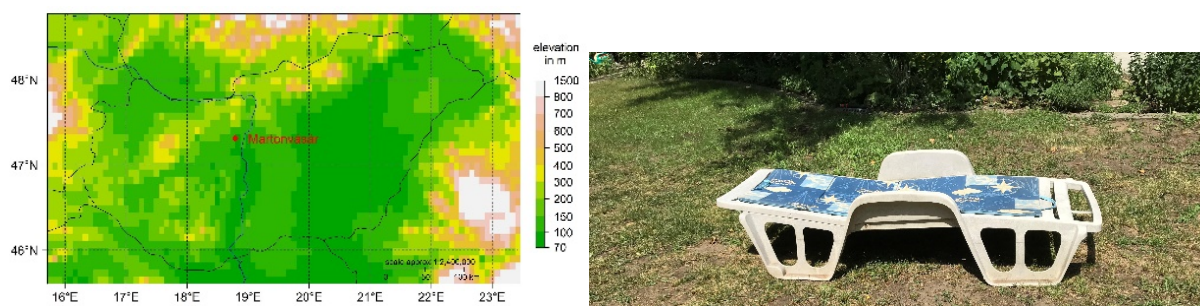

Figure 3. On the left, the location of the observation is Martonvásár, it is presented on a topographical map of Hungary. On the right, the sunbed and the beach pillow for monitoring the thermal sensation without observer in the garden of the observer's house

Martonvásár is located in the Central Transdanubian Region. This region is hilly, so the variety of meso- and microclimates is somewhat greater than in the plain areas. The Köppen method does not see this variability, but neither does the variability of summer heat supply conditions, especially in terms of human thermal load. The following observations and analyses are intended to fill this gap.

Data

Weather and human data are used.

Human data

Two human data types are used: a) data needed for identifying skin type (skin color, eye color and hair color at a young age) and b) data characterizing thermal perception type. Data for identifying skin type are presented in Table 3.

Table 3. Input variables for determining Fitzpatrick skin type and the Fitzpatrick skin type of the observer

Person	Skin color (scale 1-30)	Eye color (scale 1-16)	Youthful hair color (scale 1-10)	Sum of points	Fitzpatrick skin type and its description
Observer	7	8	8	23	IV, moderate brown skin

Thermal perception data are registered on a 7-grade scale, which contains the following grades: "very warm", "warm", "slightly warm", "neutral", "cool", "cold", "very cold". In this study, by definition, we only used the first 4 thermal perception types. The method is not applicable to cold thermal perception types. We can see that the terminology used to indicate thermal perception types is somewhat different from the commonly used terminology (Enescu, 2019). We did not distinguish between "very warm" and "unbearably warm/hot". Further discussion of human data can be found in the section Results.

Weather data

We used the following weather data: air temperature, relative humidity of air, average wind speed, wind gust speed, air pressure, relative sunshine duration and cloudiness. All the elements, except for the last two, were measured by the automatic station of the company Időkép. The data are taken from the website of the company Időkép (https://www.idokep.hu/). The beeline distance between the station and the observer's location (garden of a family house) is shorter than 3 km. Cloud cover and relative sunshine duration data are provided by the observer. Cloud cover is estimated visually in tenths. Relative sunshine duration refers to the observer's body because the human body's thermal load is to be estimated. In 2022, there were 331 observations made between May 12 and September 18. The observations not only recorded many cases, but also cases with the lowest and highest heat loads, so multi-year observations were not necessary.

Among weather elements, more attention will be paid to air temperature, incoming solar radiation and relative air humidity. The air temperature values obtained during thermal perception observations are shown in Figure 4.
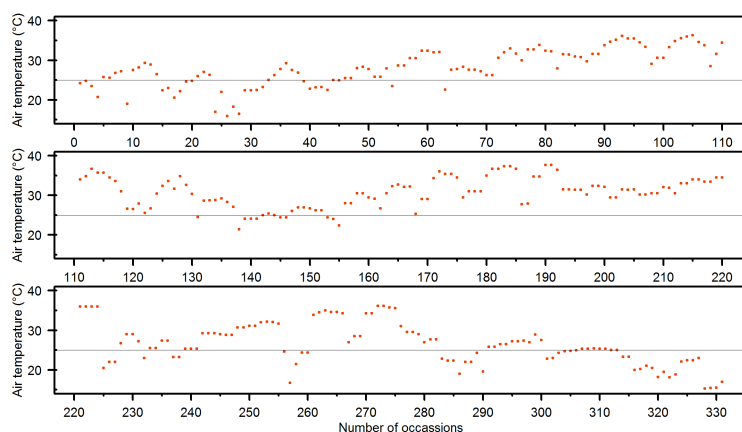
Figure 4. The air temperature values during thermal perception observations

We can see that the lowest air temperature values were around 16 °C (minimum is 15.9 °C), the highest around 37 °C (maximum is 37.2 °C). In the vast majority of the cases, air temperature was higher than 25 °C. In summer, in addition to temperature, incident solar radiation also plays a decisive role. The values of incident solar radiation estimated during the observations are shown in Figure 5.
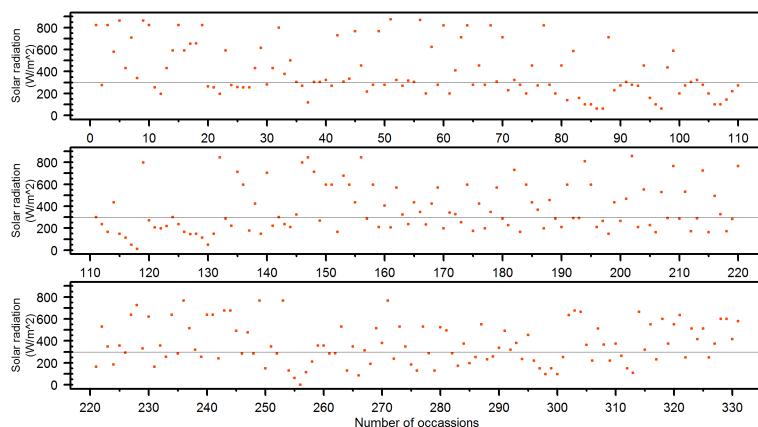
Figure 5. The incoming solar radiation values during thermal perception observations

The smallest value was 49 Wm^{-2}, the largest value was 870 Wm^{-2}. In the vast majority of cases the values exceeded 300 Wm^{-2}. Due to the estimation of skin surface evaporation, air humidity is an important input data. The evolution of these data during the observation period is shown in Figure 6.
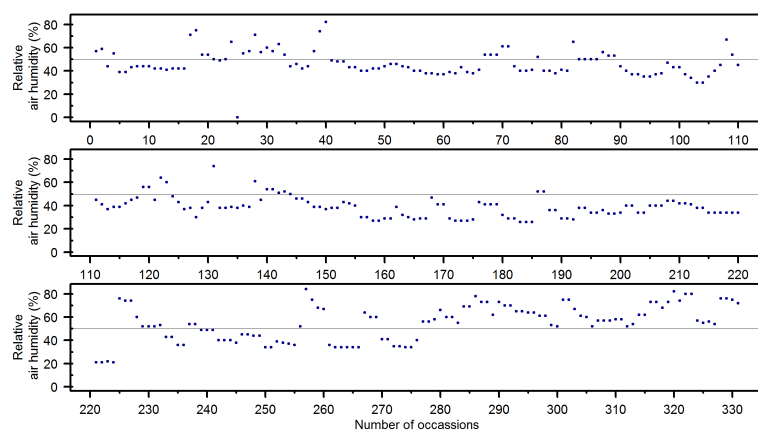
Figure 6. The relative air humidity values during thermal perception observations

The values varied between 20-80% (minimum value was 21%, maximum value was 88%), but the majority of values were below 50%. Wind speed values (not presented here) varied within wide limits. Average wind speed values varied between 0.5-8 ms^{-1}, wind gust speed values between 1.4-13.3 ms^{-1}. The highest wind speed values were in the afternoon on July 10. In the majority of the cases, average wind speed varied between 1.5-3 ms^{-1}.

Results

Several results are presented and discussed. Firstly, we give some basic information regarding M and the skin type of the observer. After this we characterize the relationship between λE_{tot} and operative temperature as well as the relationship between thermal perception types and λE_{tot}. The relationship between r_{skin} and operative temperature is also presented and analysed. Finally, we examined the sensitivity of λE_{tot} to changes in skin albedo and we will talk also about the applicability of the model.

Observer's M value and skin type

When choosing the observer's M value of, we took into account the values of the observer's heart rate (58-65 BPM (beats per minute)), as well as the value range of resting metabolic heat flux density (M_r) (ISO8996, 2004). M_r's range is 55-70 Wm^{-2}. The M_r value of the observer was chosen to be low, because his resting heart rate values are lower. Based on the information presented in Tables 2 and 3, the observer's skin type is skin type IV on the Fitzpatrick skin type scale. The skin color characterization of this skin type is "Mediterranean, Hispanic". This additional information about skin type is given because we made thermal perception observations.

Relationship between skin evaporation and operative temperature

The scatter chart of λE_{tot}–T_o relationship is presented in Figure 7.
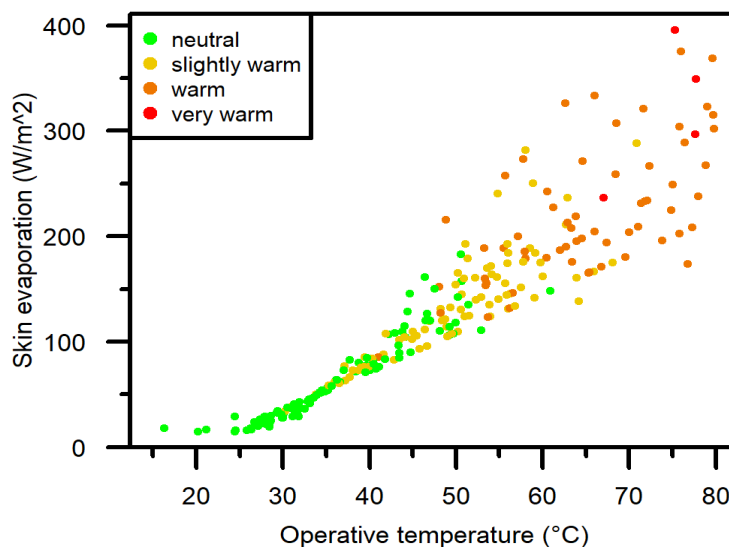

Figure 7. Scatter chart of the latent heat flux density of skin surface evaporation as a function of operative temperature at actual average air humidity and wind speed. Thermal perception types experienced during the observations can also be seen based on the coloring of points

λE_{tot} is the sum of evaporation from dry skin λE_{ds} and sweaty skin λE_{sw}. It should be mentioned that λE_{sw} can be estimated as the difference between λE_{tot} and λE_{ds}. λE_{ds} can be parameterized, for instance, as a function of T_{skin} (Parsons, 2003). The point cloud can be

divided into 2 parts. In the range 25 °C < T_o < 45 °C, the change of λE_{tot} as a function of T_o can be considered linear, the maximum values of λE_{tot} are around 100 Wm^{-2}, the thermal perception types are "neutral" (smaller T_o) and "slightly warm" (larger T_o). In the range 45 °C < T_o < 80 °C, the scatter of the points is significant, and the amount of scatter increases with increasing T_o. The maximum values of λE_{tot} are around 300-400 Wm^{-2}. For T_o = 70 °C, λE_{tot} is scattered between 170 and 320 Wm^{-2}. We can see that in the case of thermal perception types "warm" and "very warm", the points characterizing the λE_{tot}-T_o relationship are irregularly scattered and cannot be characterized by a regression relationship.

Relationship between thermal perception types and skin evaporation
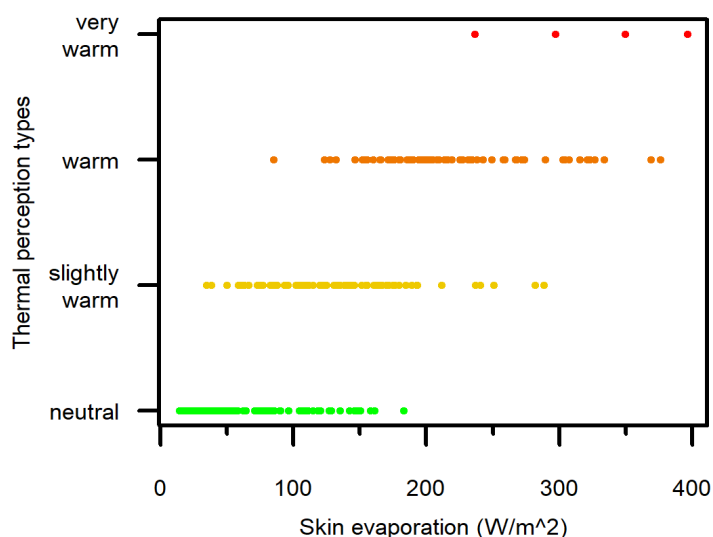The relationship between thermal perception types and λE_{tot} is presented in Figure 8.

Figure 8. Scatter chart of thermal perception as a function of latent heat flux density of skin surface evaporation

In the range 20 Wm^{-2} ≤ λE_{tot} < 160 Wm^{-2} (except for 1 observation), thermal perception type is "neutral". In the range 50 Wm^{-2} ≤ λE_{tot} < 200 Wm^{-2} (except for 8 observations), thermal perception type is "slightly warm". It can be seen that there is a large overlap between the thermal perception types "neutral" and "slightly warm". Thermal perception type "warm" appeared in the range 130 Wm^{-2} ≤ λE_{tot} < 340 Wm^{-2} (except 3 observations). Thermal perception type "very warm" is becoming to be typical in the range 340 Wm^{-2} < λE_{tot}. This range is the same as the T_o ≥ 75-80 °C range. Note that we did not distinguish between thermal perception types "very warm" and "hot" or "unbearably hot". These latter thermal perception types occur when air temperature is at least 25 °C and incoming solar radiation is at least 700 Wm^{-2}.

Relationship between evaporative resistance of skin and operative temperature
The scatter chart of evaporative skin resistance–operative temperature relationship is presented in Figure 9.
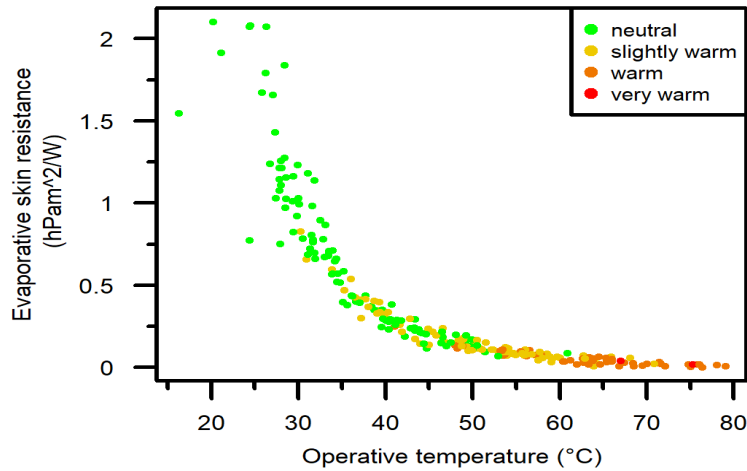
Figure 9. Scatter chart of the evaporative skin resistance as a function of operative temperature at actual average air humidity and wind speed. Thermal perception types experienced during the observations can also be seen based on the coloring of points

Each point in the figure represents an observation. The change of r_{skin} as a function of T_o is clearly visible. The points can be approximated by the following exponential function:

$$r_{skin} = 19.17 \cdot e^{-0.1017 \cdot T_o}.$$

In the range 30 °C $\leq T_o <$ 35 °C, r_{skin} decreases sharply with increasing T_o. The perceived thermal sensation type is mostly "neutral". In the range 35 °C $\leq T_o <$ 50 °C, the rate of reduction of r_{skin} with increasing T_o is much smaller than in the former case. The thermal sensation types are mostly "slightly warm" and "neutral". A reduction of r_{skin} as a function of T_o can still be observed in the range 50 °C $\leq T_o <$ 70 °C. The thermal perception types are mostly "slightly warm" and "warm". In this range, the thermal perception type "very warm" was also registered once. In the range 70 °C $\leq T_o$, the reduction of r_{skin} as a function of T_o is practically negligible, r_{skin} can be taken as constant, its value is equal to or less than 0.005 hPa·m^2·W^{-1}. In this range, the thermal perception type "very warm" appears and its frequency increases considerably with increasing T_o.

Sensitivity of skin evaporation and evaporative resistance of skin to skin albedo
The comparison of λE_{tot} values for lower (0.13) and higher (0.27) skin surface albedo values is shown in Figure 10.
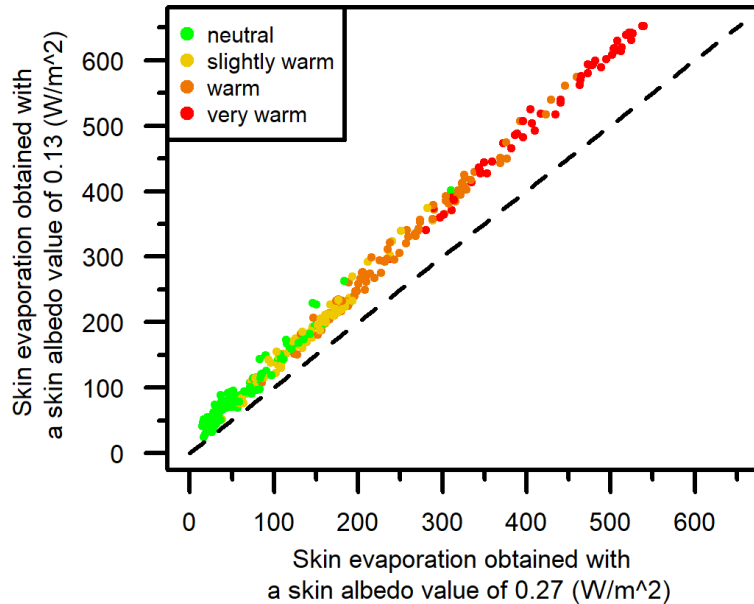
Figure 10. Scatter chart of latent heat flux density of skin evaporation simulated by lower (albedo value 0.13) and higher (albedo value 0.27) skin albedo values. Thermal perception types experienced during the observations can also be seen based on the coloring of points

Since λE_{tot} is calculated as the residual term of the energy balance equation, it makes sense that $\lambda E_{tot}^{0.13} > \lambda E_{tot}^{0.27}$. The $\lambda E_{tot}^{0.13} - \lambda E_{tot}^{0.27}$ differences increase with increasing λE_{tot} moving towards warm thermal perception types. Thus, for instance, in the thermal perception type "very warm", $\lambda E_{tot}^{0.13} - \lambda E_{tot}^{0.27}$ differences are around 100 Wm^{-2}. This change is also beautifully reflected in the ratio of r_{skin} values (Figure 11).

INTERNATIONAL
SCIENTIFIC
JOURNAL

GEOGRAPHICA
PANNONICA

Ferenc Ács, Erzsébet Kristóf, Annamária Zsákai
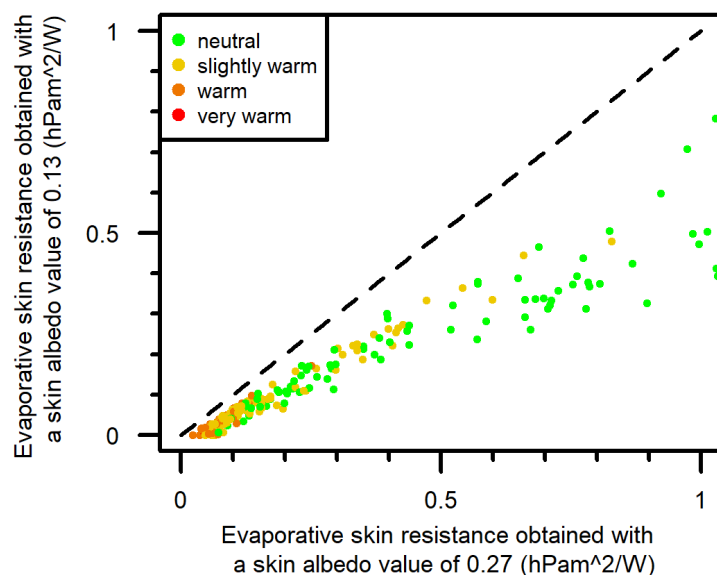Geographica Pannonica | Volume 29, Issue 4, 282-300

Figure 11. Scatter chart of the skin evaporative resistance simulated by lower (albedo value 0.13) and higher (albedo value 0.27) skin albedo values. Thermal perception types experienced during observations can also be seen based on the coloring of points.

Based on the model, it makes sense that $r_{skin}^{0.13}$ is smaller than $r_{skin}^{0.27}$ because $\lambda E_{tot}^{0.13}$ is larger than $\lambda E_{tot}^{0.27}$. It can be seen that the $r_{skin}^{0.13}/r_{skin}^{0.27}$ ratio decreases moving from the thermal perception type "very warm" to the thermal perception type "neutral". This ratio is the smallest when the thermal perception type is "neutral". This ratio is higher in the "warm-neutral" situations and lower in the "cold-neutral" situations. The "warm-neutral" thermal perception type is the "slightly warm" side of the "neutral" thermal perception type, and conversely, the "cold-neutral" thermal perception type is the "cool" side of the "neutral" thermal perception type. Note that $r_{skin}^{0.27}$ is almost double of $r_{skin}^{0.13}$ in the thermal perception range "cold-neutral". It is interesting to see that the albedo value of the skin surface determines the magnitude of evaporative resistance (r_{skin} value) when the thermal sensation type is "neutral".

Applicability of the model
By definition, the model cannot be applied if the r_{skin} value is negative. This can happen in two cases: when 1) the first term of eq. (4) is smaller than the r_{Ha} term and when 2) the first term of eq. (4) has a negative sign. The first case occurs when the R_n values are very large; the second case occurs when the R_n values are very small. In both cases, incoming solar radiation is a determining factor. When solar radiation is high, above 700 Wm^{-2}, the R_n values are around 400 Wm^{-2}, and when wind speed is lower or moderate, the first term of eq. (1) will be smaller than the r_{Ha} term. Of course, air temperature is at least around 20-25 °C. In these cases, the thermal perception type "very warm" is the most common. When solar radiation is low, about 100 Wm^{-2}, or even smaller, R_n values can be around 0 or even negative, and thus

the denominator of the first term of eq. (4) can become negative. In such cases, the thermal perception type is "neutral".

Discussion

The presented model is obviously simple. It uses the concept of required sweating (Parsons, 1997) as well as the evaporation gradient formula. The use of the gradient formula is also an important part of the model, so we can also estimate the value of the skin surface evaporative resistance, which is naturally always greater than or equal to zero. With this methodological innovation, we have made the concept of required skin surface evaporation completely universal, as the concept not only fulfills the energy balance, but also the physical laws characterizing the transfer of water vapor (Monteith, 1965). Another unique feature of the model is that the active surface is the skin surface (not the clothing surface). Therefore, we preferred to look at a person in a lying position. Thanks to this, human variability is not determined by the variability of metabolic heat flux density values, but by the variability of skin types. That's why it was important to specify the skin type of the person suffering from heat stress.

Nowadays, only fewer studies link information from climate type and human thermal load (e.g. Yang & Matzarakis, 2019; Blazejczyk et al., 2015; Ács et al. 2020; Ács, 2024). In all of these studies, the persons, or the "standard human" wear clothing, i.e., the active surface used in the model is the clothing surface. To the best of our knowledge, the skin surface has not yet been used as an active surface. It should be emphasized that, according to Monteith (1965), every surface type has an evaporative resistance value. From this perspective, our approach is entirely justifiable - even if it is not common. Due to the above, our results are new and provide a human-based characterization of the summer weather conditions of the Cfb climate. The λE_{tot} values varied between 10 and 300-350 Wm^{-2}, meanwhile 25 °C < T_o < 80 °C. It should also be noted that the simulated λE_{tot} results were not verified by comparing them with other measurement or model calculation results. However, the λE_{tot} results were always compared with the observed thermal sensation type results, and their consistency was perfect. Note, when T_o is around 35 °C (we referred to this as a "warm neutral" thermal sensation), the λE_{tot} values are around 50 Wm^{-2}. In these cases, λE_{sw} is comparable with λE_{ds}. Of course, we are aware that the λE_{tot}-thermal sensation type relationship could be very individual. It is more individual than the clothing resistance-thermal sensation relationship (Ács et al., 2022), since this relationship also depends on skin type.

As a fact, we can state that only results of one observer are presented. This can even be considered as a serious shortcoming. We tried to compensate for this deficiency by specifying the observer's skin type. Based on this, it is obvious that observations of people with other skin types are also needed for the method to be used more generally. At the same time, it should also be emphasized that, to the best of our knowledge, this longitudinal research is the first of its kind.

Finally, the study – both its methodology and its results – brings people closer to outdoor conditions characterized by sunlight, primarily through understanding the relationship between thermal load and thermal perception. This type of awareness encourages a healthier lifestyle, which is also proclaimed globally by the United Nations, see SDG (Sustainable Development Goals) 3 entitled as "Ensure healthy lives and well-being for all at all ages". The study and its results also raise awareness of the importance of self-knowledge. In this regard, it is also worth mentioning that the Fitzpatrick skin type test is considered a standard skin type test method.

Conclusion

In this study, the active surface is the skin surface of the human body, as the clothing worn is minimal in accordance with behavioral norms. Accordingly, we observed a lying person whose body is under the influence of excess heat caused by the summer weather conditions of the Cfb climate. According to the results of a new model based on the human body energy balance equation and the skin surface evaporation gradient formula, the following main conclusions can be drawn: 1) The concept of "required skin evaporation" can be successfully applied to quantitatively characterize human heat excess by linking „required skin evaporation" and thermal perception information. 2) Since the albedo of the skin surface depends on the skin type, the "required skin evaporation" concept (calculation of λE_{tot} and r_{skin}) is more sensitive to higher than lower thermal loads.

It should be emphasized that the application of the concept does not require the parameterization or characterization of thermoregulatory processes.

References

Ács, F. (2024). On the Comparison of Generic and Human-based Climate Classification Methods. *Research Advances in Environment, Geography and Earth Science*, *7*, 64–78. https://doi.org/10.9734/bpi/raeges/v7/1631

Ács, F., Kristóf, E., & Zsákai, A. (2025) (in press). Human thermal load of foggy and cloudless mornings in the cold season. *Geofizika*, 42.

Ács, F., Zsákai, A., Kristóf, E., Szabó, A. I., & Breuer, H. (2020). Carpathian Basin climate according to Köppen and a clothing resistance scheme. *Theoretical and Applied Climatology, 141*, 299–307. https://doi.org/10.1007/s00704-020-03199-z

Ács, F., Zsákai, A., Kristóf, E., Szabó, A.I., & Breuer, H. (2022). Individual local human thermal climates in the Hungarian lowland: Estimations by a simple clothing resistance-operative temperature model. *International Journal of Climatology*, *43*(3), 1273–1292. https://doi.org/10.1002/joc.7910

Basarin, B., Lukić, T., & Matzarakis, A. (2020). Review of Biometeorology of Heatwaves and Warm Extremes in Europe. *Atmosphere*, *11*(12), 1276. https://doi.org/10.3390/atmos11121276

Bátori, L. (2022). Examination of the impact of climate change on sport on the example of the heat index. In International Conference *National Higher Education Environmental Science Student Conference*, June 3-5, Shanghai.

Błażejczyk, K., Baranowski, J., Jendritzky, G., Błażejczyk, A., Bröde, P., & Fiala, D. (2015). Regional features of the bioclimate of Central and Southern Europe against the background of the Köppen-Geiger climate classification. *Geographia Polonia*, *88*, 439–453. 10.7163/GPol.0027

Bokros, K., & Lakatos, M. (2022). Analaysis of hot spells in Budapest from the early 20th century to the present. *Légkör, 67*(4), 208–218. (in Hungarian)

Boras, M., Herceg-Bulić, I., Zgela, M., & Nimac, I. (2022). Temperature characteristics and heat load in the City of Dubrovnik. *Geofizika, 39*(2), 259–279. https://doi.org/10.15233/gfz.2022.39.16.

Brunt, D. (1932). Notes on radiation in the atmosphere. *Quaterly Journal of Royal Meteorological Society, 58*(247), 389–420.10.1002/qj.49705824704.

Campbell, G. S., & Norman, J. M. (1997). *An introduction to environmental biophysics* (2nd ed.). Springer.

Enescu, D. (2019). Models and Indicators to Assess Thermal Sensation under Steady-State and Transient Conditions. *Energies*, *12*(5), 841. https://doi.org/10.3390/en12050841

Fanger, P. O. (1970). *Thermal comfort: Analysis and applications in environmental engineering*. Danish Technical Press.

Fitzpatrick, T. B. (1975). "Soleil et peau" [Sun and skin]. *Journal de Médecine Esthétique* (in French), *2*, 33–34.

Fouilett, A., Rey, G., Laurent, F., Pavillon, G., Bellec, S., Guihenneuc-Jouyaux, C., Clavel, J. Jougla, & E. Hemon D. (2006). Excess mortality related to ´ the August 2003 heat wave in France. *International Archives of Occupational and Environmental Health*, *80*(1), 16–24.

Gulyás, Á. & Matzarakis, A. (2009). Seasonal and spatial distribution of physiologically equivalent temperature (PET) index in Hungary. *Időjárás, 113*(3), 221–231.

Hantel, H., & Haimberger, L. (2016). *Grundkurs Klima*. Springer Spektrum. https://doi.org/10.1007/978-3-662-48193-6

ISO 8996. (2004). *Ergonomics of the thermal environment – Determination of metabolic rate* (2nd ed.). International Organization for Standardization.

Khosla, R., & Guntupalli, K.K. (1999). Heat-related illnesses. *Crit Care Clin, 15*(2), 251–263. 10.1016/s0749-0704(05)70053-1

Konzelmann, T., van de Wal, R. S., Greuell, W., Bintanja, R., & Henneken, E. A. (1994). Abe-Ouchi, A. Parameterization of global and longwave incoming radiation for the Greenland Ice Sheet. *Global Planetary Change, 9*(1-2), 143–164. 10.1016/0921-8181(94)90013-2.

Kottek, M., Grieser, J., Beck, C., Rudolf, B., & Rubel, F. (2006). World Map of the Köppen-Geiger classification updated. *Meteorologische. Zeitschrift*, *15*(3), 259–263.

Kovács, A., Németh, Á., Unger, J., & Kántor, N. (2017). Tourism climatic conditions of Hungary – present situation and assessment of future changes. *Időjárás*, *121*(1), 79–99.

Köppen, W. (1900). Versuch einer Klassifikation der Klimate, vorzugsweise nach ihren Beziehungen zur Pflanzenwelt. *Geographische Zeitschrift*, *6*(11), 593–611.

Köppen, W. (1936). *Das geographische System der Klimate*. Gebrüder Borntraeger.

Matzarakis, A., & Gulyás, Á. (2006). A contribution to the thermal bioclimate of Hungary: Mapping of the physiologically equivalent temperature. In A. Kiss, G. Mezősi, & Z. Sümeghy (Eds.), *Landscape, environment and society: Studies in honour of professor Ilona Bárány-Kevei on the occasion of her birthday* (pp. 479–488). University of Szeged.

Matzarakis, A., Rudel, E., Zygmuntowski, M., & Koch, E. (2005). Thermal Human Bioclimate Conditions for Austria and the Alps. *Croatian Meteorological Journal*, *40*, 190–193.

Megyeri-Korotaj, O.A., Bán, B., Suga, R., Allaga-Zsebeházi, G., & Szépszó, G. (2023). Assessment of Climate Indices over the Carpathian Basin Based on ALADIN5.2 and REMO2015 Regional Climate Model Simulations. *Atmosphere*, *14*, 448, https://doi.org/10.3390/

Mieczkowski, Z.T. (1985). The tourism climatic index: a method of evaluating world climates for tourism. *Canadian Geographic*, 29, 220–233.

Mohan, M., Gupta, A. & Bhati, S. (2014). A modified approach to analyse thermal comfort classification. *Atmospheric and Climate Sciences*, 4, 7–19. 10.4236/acs.2014.41002

Monteith, J. L. (1965). Evaporation and environment. In *Proceedings of the 19th Symposium of the Society for Experimental Biology* (pp. 205–236). Cambridge University Press.

Nielsen, K. P., Zhao, L., Stamnes, J. J., Stamnes, K., & Moan, J. (2008). The optics of human skin: Aspects important for human health. In E. Bjertnes (Ed.), *Solar radiation and human health* (pp. 35–46). The Norwegian Academy of Science and Letters.

Páldy, A., Bobvos, J., & Málnási, T. (2018). The impact of climate change on human health and health care system in Hungary. *Magyar Tudomány*, *179*(9), 1336–1348. 10.1556/2065.179.2018.9.7

Parsons, K. C. (2003). *Human thermal environments* (2nd ed.). Taylor & Francis.
Parsons, R. A. (1997). Evaporative heat loss from skin. In *1997 ASHRAE Handbook* (Chapter 8: Thermal Comfort, p. 8.3). Frank M. Coda.

Potchter, O., Cohen, P., Lin, T.P., & Matzarakis, A. (2018). Outdoor human thermal perception in various climates: a comprehensive review of approaches, methods and quantification. *Science of The Total Environment*, 631–632, 390–406. 10.1016/j.scitotenv.2018.02.276

von Humboldt, A. (1845). *Kosmos: Entwurf einer physischen Weltbeschreibung* [Cosmos: A sketch of the physical description of the universe] (in German). Cotta.

Yang, S.Q., & Matzarakis, A. (2016). Implementation of human thermal comfort information in Köppen-Geiger climate classification— the example of China. *International Journal of Biometeorology*, *60*, 1801–1805. 10.1007/s00484-016-1155-6